An Investigation on the Shape Factors of Aggregates

D.H.H.P. Dassanayake[1]*, N. Ahilash[1],A.J.M.S.D. Premasiri[1],H.G.H.N. Jayasekara[1] and D.N. Subramaniam[1]

[1]Department of Civil Engineering, Faculty of Engineering, University of Jaffna, Ariviyal Nagar, Kilinochchi, SRI LANKA

Abstract

The aggregate properties such as aggregate size distribution and aggregate shape distribution, affect the mechanical performance of concrete. Although shape of aggregates are computed using various computational methods in researches, it was not clear, which of them define the shape of an aggregate as a whole. This study aims to investigate the shape factors (two-dimensional) in defining the shape of an aggregate. Aggregates of size between 5 – 30 mm diameter were obtained from different batches of aggregate samples that underwent treatment of varied degrees of revolutions in LAAV. Fourteen different shape factors were quantified using image analysis techniques and were tested for ANOVA, regression, principal components and correlation analyses. No shape factor defined the shape of an aggregate individually, while several shape factors were highly correlated. A combination of at least three shape factors is required to define the shape of an aggregate numerically.

Keywords— *Aggregate shape,shape factors,aggregate packing,packing density,aggregate size distribution*

Introduction

The composition and characteristics of coarse aggregates play a pivotal role in shaping the properties of concrete, yielding both quantity and quality aspects that define the performance of the resulting material. However, the extraction process of aggregates exacts an environmental disturbance due to the depletion of non-renewable resources and the geographical implications of extraction [1]. Current challenge is the economic sustainability of this industry, prompting explorations into alternative materials as part of contemporary research endeavors. The optimization of aggregate utilization through concrete mix design, with a focus on enhancing efficiency and reducing required cement paste – termed packing optimization – has been a dominant pursuit [2]. In this objective, packing density emerges as a pivotal determinant of material strength, urging engineers to optimize it.

While the distribution of aggregate sizes is a significant influence on packing within a concrete mold, the role of aggregate shape and its distribution cannot be understated [3]. Yet, despite the development of packing models for mono-size and binary-size particles, the packing involving size distributions remains largely unexplored. As the influence of aggregate size distribution on aggregate packing is established, the additional impact of aggregate shape further complicates the packing density landscape.

Incorporating aggregate shape quantitatively into packing models necessitates assigning a numerical value to aggregate shape. Although computational methods to define aggregate shape have been deployed in various contexts, the comprehensive characterization of these shape factors and their effectiveness in predicting material performance has not been sufficiently addressed. Notably, a range of studies have focused on the definition of aggregate shape through computational methods, including the context of powder technology [4] and geotechnical engineering applications [5].

However, certain gaps remain in understanding how these shape factors correlate with particle size distributions and how they contribute to aggregate packing density. Historically, the early 1930s saw initial attempts to incorporate shape factors alongside aggregate size to define packing density[6, 7]. Notably, the majority of studies have concentrated on specific particle mixtures, with a focus on monosized and binary particle mixtures[8, 9]. Additionally, while technological advancements have enabled shape factor analysis through Digital Image Processing (DIP) techniques, challenges remain in effectively integrating three-dimensional data into the analysis[10].

This study sets out to address these knowledge gaps and contribute to the existing body of research. Specifically, the research objectives driving this investigation are: available shape factors identified in previous literature, variation of different shape factors based on the particle size distribution, identification of the interrelation between shape factors and revolutions. Through a meticulous exploration of these research questions, this study aims to unravel the intricate relationship between aggregate shape, packing density, and material performance. By exploring

*Corresponding author: 2018e024@eng.jfn.ac.lk
Received: March 16, 2023, **Published:** October 06, 2023

into this uncharted territory, this research seeks to illuminate insights and pave the way for more informed decision-making in concrete mix design and application.

Shape is external morphology of particles that can visually be observed while experimental and numerical depiction of shape is vital in model development. While several computational methods were used to define the shape of aggregates in different contexts, studies have not characterized these shape factors and identifying the efficacy of the numerical value in predicting the performances of resulting packed materials. This study aims to identify and characterise shape factors, available in literature, specifically in the context of aggregates in the range of $5 - 25$ *mm* diameter.

Materials and Methods

In this study, crushed aggregates were used as raw material and they were obtained from local quarry in Northern Province, Sri Lanka. The particle sizes of aggregates used in this study ranged between1/2" (12 *mm*) to 1" (25 *mm*). Another sample of aggregates (bigger than 12 *mm*) were obtained from aggregate pool and were separated into nine batches. Based on the principal of abrasion, when aggregate particles undergo abrasion, the smoothness and shape of particles change significantly. With the intention of producing aggregates of same size, but with different shapes, each batch of aggregates were then processed in LAA (Los Angeles Abrasion) machine (ball milling) for different amount of revolutions, ranging from 50 to 2000 revolutions (50, 100, 150, 200, 400, 500, 1000, 1500 and 2000). After 2000 revolutions the whole sample was recognized as almost dust, no coarser particles were identified. Each batch of samples (nine) were then sieved with 25 *mm* and then 12 *mm* sieves and particles sizes between $12 - 25$ *mm* diameter were selected. The samples were then washed in tap water and left to dry in air for 24 hours. Two batches of aggregates that had zero and 1000 revolutions treatment in LAAV are shown in Figure 1.

Specific amount of coarse aggregate samples was taken and coloured in black paint. They were then allowed to dry in room temperature. After drying, those particles were spread on a white sheet with A4 area on the special arrangement. An image of arranged sample was taken by covering completely white sheet. Arranged particles were mixed together, rearranged on the sheet and images were taken again. This procedure was repeated 12 times and 12 different images were obtained.

Particle size distributions of the aggregates, which

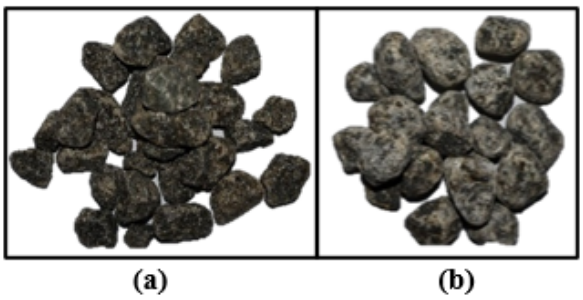

Figure 1: *Batch of aggregates that were (a) not treated and (b) treated in LAAV (1000 revolutions)*

were used in this study, were determined by image analysis method. The analysis was performed using ImageJ, an open-source software designed for processing and analyzing scientific images. To begin, the images were cropped against a white background and subsequently converted into a binary scale (black and white) within the software. This step followed the appropriate image scaling. The binary images were then subjected to processing, resulting in the isolation of black zones representative of the aggregate surface area. The diameters of these white zones were measured, and corresponding boundaries was generated.

This approach enabled the determination of cumulative aggregate percentages, which, in turn, facilitated the creation of a particle size distribution curve. Furthermore, to enhance the accuracy of analysis, we referred to established shape factors outlined in the existing literature. These shape factors were meticulously computed for the aggregates under investigation, as outlined in Table 1. The dimensional parameters integral to the calculation of these shape factors are detailed below.

Bounding rectangle is the smallest rectangle enclosing the selection. This dimension called as breadth and height in ImageJ as shown in Figure 2 (a).

Fit Ellipse is known as the best fitting ellipse for this area. For this method, primary axis and secondary axis lengths were need, which are shown as Minor and Major in ImageJ as shown in Figur 2 (b).

There are two Feret's dimensions. It measures the size of an area along a specified direction as shown in Figure 2 (c). Feret is the longest distance between any two points of the section boundary. (Maximum Caliper) MinFeret is the smallest distance between any two points of the section boundary. (Minimum Caliper)

The other raw data were analyzed by using Microsoft Excel 2019 and shape factor values were also obtained from Microsoft Excel 2016 using the equations and dimensions given above. The variations were visually analysed using graphical analyses while statistical analyses were carried out using SPSS

Table 1: *Descriptions of shape factors used in this study*

	Shape Factor	Computation		Shape Factor	Computation
J.C	ImageJ circularity	$\frac{(4\pi\ area)}{(perimeter)^2}$	SF.FR	Sneed and Folk flatness ratio	$\frac{Breadth}{Length}$
J.AR	ImageJ aspect ratio	$\frac{majoraxis}{minoraxis}$	FAR	Feret's aspect ratio	$\frac{Feret}{MinFeret}$
J.R	ImageJ roundness	$\frac{4\pi\ area}{\pi\times(majoraxis)^2}$	SF	Shape factor	$\frac{Perimeter}{Calculatedperimeter}$
J.S	ImageJ solidity	$\frac{area}{convexarea}$	PSC	Projected sphericity/circularity	$\frac{D.Calculated}{Feret}$
KS	Krumbein sphericity	$\sqrt[3]{\frac{breadth}{length}}$	ICS	Inscribed circle sphericity	$\sqrt{\frac{MinFeret}{Feret}}$
BSF	Barksdale et al. shape factor	$\frac{length}{(breadth)^2}$	C	Circularity	$\frac{(perimeter)^2}{area}$
FR	Kwan and Mora fullness ratio	$\sqrt{\frac{area}{convexarea}}$	PS	Projected sphericity	$\frac{area}{AC}$

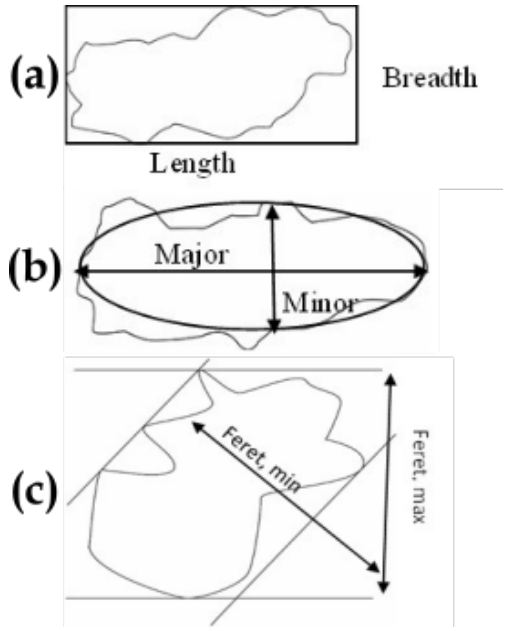

Figure 2: *(a) Length and breadth of aggregate particle (b) Major and minor axes of an aggregate particle (c) Feret dimensions of an aggregate*

and MiniTab 2019. Thereafter, the relationship in between shape factors and the relationship between particles size distribution and shape factors were obtained. Finally, cluster analysis was carried out based on the similarity between shape factors and the shape factors that best represented the shape of aggregates were presented.

Aggregates for the experiment purchased as a single batch. Aggregates were colored by maintaining the thin layer. Because the shape of the aggregate holds significance in the analysis, it is imperative to ensure that the aggregate's shape remains unchanged throughout the process. The images of the aggregates were taken from the top. The aperture was set of $f/9.0$ to decrease the blur effect and ISO and shutter speed were set 800 and $1/250\ s$ throughout the imaging process. To maintain constant image quality, a special setup is used. The camera was fixed in the top and the images were taken from the constant

Figure 3: *Special setup used for image capturing and Digital Image processing (Binary Result)*

height and centre. Special setup used for image capturing and Digital Image processing (Binary Result) is shown in Figure 3

Results and Discussion

Particle Size Distribution and Shape Factors

The particle size range and distribution of all samples used in this study had a consistent range and distribution, as shown in Figure 4. The particle sizes varied between 5 mm and 30 mm, with a D_{50} of approximately 18 mm. The consistency of this observation across all samples ensured that the size imparted no variation on the analyses on the shape of aggregates.

As discussed in the methodology, the shape factors were computed from the images of the aggregates. Analysis of Variance (ANOVA) was conducted on each shape factor to understand if aggregates with different treatments in LAAV had clustered. Figure 5

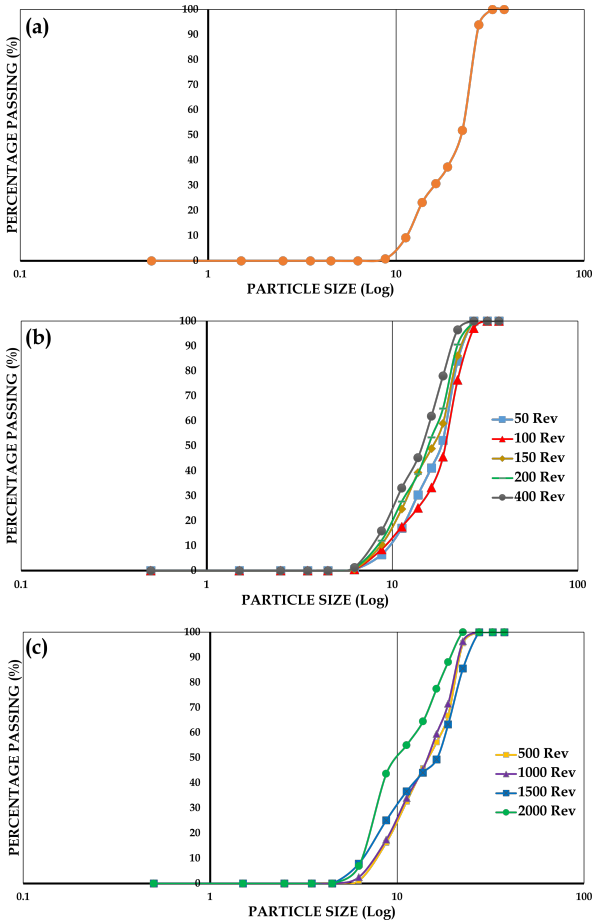

Figure 4: *Particle size distribution of aggregates with (a) zero revolutions, (b) 50 - 400 revolutions and (c) 500 - 2000 revolutions*

shows the clusters as identified from ANOVA test (the classes that had significant difference based on the number of revolutions), individually done for ten shape factors. It is evident from the figure that shape factors had significantly different measures of the shape of aggregates. The shape factors J.S, FR, SF.FR, ICS and PS have no patterned grouping from the ANOVA test. Feret diameters encountered shape factors and convex area encountered shape factors have no patterned grouping. Even though, other Bounding rectangle property involves for Krumbein Sphericity, Barksdale Shape factor etc. have a grouping pattern, Flatness ratio have no identical grouping pattern.

The results obtained from Figure 6 demonstrate that the utilization of bounding Rectangle, fit ellipse, or Feret property methods induce impact in shape factor properties. Although the shape factors identify significant difference between batches of aggregates, some have a higher degree of distinguishability compared to other shape factors. Certain shape factors, such as FAR, SF, and C, exhibit greater distinguishability at lower revolutions, while other shape factors like BSF and SF demonstrate enhanced distinguishability at higher revolutions.

Table 2: *Summary of variance explained by three principal components*

Component	% of variance	Cumulative
1	49.2	49.2
2	29.3	78.5
3	11.7	90.2

Lower revolutions predominantly smoothens the surface of the aggregates due to abrasion, rather than effecting significant changes in the macro structure of the aggregate, while higher revolutions affect the macro-shape of the aggregate. Therefore, shape factors indicate measurements of different scales of shape. Further analyses are required to understand the combinations of shape factors that can define the shape of an aggregate emphatically.

From Figure 6 shows the shape factors have same mean trend and revolutions of LAAV. In the observed data, it's apparent that certain shape factors exhibited changes with revolutions (alterations in aggregate shape), whereas several other shape factors remained relatively stable. Clearly, FAR, J.AR, SF, and C displayed negative correlations with revolutions, whereas all other shape factors displayed positive correlations. In addition to the trends, the figure also shows that there are few shape factors behave very similar to a few other factors. Further analyses on similarity is required to identify the similar shape factors.

Figure 7 illustrates the similarity of shape factors through the clustering of aggregates using the labeled classes. J.AR, FAR, SF, C and BSF a closely related compared to other shape factors, as evident from the figure. Furthermore, it is evident that several shape factors are very similar, for example J.S and FR, J.R and ICS, PSC and PS, J.AR and FAR and SF and C. Without using these clusters, the predictive analysis conducted in Minitab. Through this predictive analysis, it becomes possible to forecast the area of the aggregate, with an optimal correlation coefficient (R) value of 0.9809.

The data matrix of 14 dimensions (14 shape factors) could be reduced in dimensionality using a Principal Component Analysis (PCA). A PCA revealed that the variance of the data matrix could be explained with 3 principal components)approximately 90% of the variance explained). Table 2 shows the percentage of variance explained by each principal component and the cumulative percentage of the first three principal components.

While the first principal component (PC) explains almost half the variance, the second PC explains another 30%. That is, the first two PCs explain 70% of the variance of the complete data matrix.

Table 3: *Summary of principal components rotated around varimax*

Shape Factor	Principal Component		
	1	2	3
J.C	0.52	0.79	0.22
J.AR	-0.93	-0.24	-0.06
J.R	0.94	0.20	0.03
J.S	0.04	0.92	-0.27
KS	0.56	-0.05	0.71
BSF	-0.32	-0.06	0.90
FR	0.04	0.92	-0.26
SF.FR	0.81	0.01	0.13
FAR	-0.94	-0.24	-0.06
SF	-0.50	-0.79	-0.24
PSC	0.88	0.40	0.00
ICS	0.95	0.22	0.04
C	-0.49	-0.78	-0.25
PS	0.87	0.40	0.00

Table 3 shows the summary of shape factors with respect to the first three PCs obtained from the PCA. It could be observed that the first PC is dominated by J.AR, J.R, SF.FR, FAR, PSC, ICS and PS. This means that these shape factors are closely related to each other in explaining the variance of the data matrix. The second PC is dominated by J.C, J.S, FR, SF and C, indicating a close correlation between them. The third PC is dominated by the remaining shape factors, KS and BSF, which explained 11% of the variance in the data matrix.

It is required to do a correlational analysis on shape factors to understand the correlation between them. A bivariate Pearson's correlation analysis is done and Table 4 shows the summary of correlation analysis. Cells highlighted in green show very high correlation coefficient (greater than 0.9) while the cells highlighted in red show insignificant correlation (less than 0.5). High correlation observed between J.S-FR, C-SF, PS-PSC, J.AR-FAR, J.R-ICS, ICS-PSC, PS-ICS, J.R-PSC and J.R-PS. These observations are quite similar to the observations in similarity analysis shown in Figure 7.

Pearson's correlation assumes a linear correlation. A lower value in correlation coefficient in Pearon's test does not imply no correlation at all, where as a non-linear correlation may be present. It is therefore important to analyse shape factors with non-linear models to understand the similarity and correlations between the shape factors.

Conclusion

This study analyses the shape of aggregates with regards to the shape factors Fourteen methods used in the literature to numerically represent the shape of an aggregate has been investigated in this study. Aggreegates were processed in LAAV instrument for different number of revolutions to effect changes in the shape of the aggregates, and the shapes of which were analysed using image analysis techniques. The following conclusions were made.

1. The ANOVA test grouped sample batches based on significant differences among shape factors. While J.S, FR, SF.FR, ICS, and PS showed no significant grouping, others did. However, no group identified all ten batches as significantly different. J.C, K.S, SF, and C grouped batches into seven categories, while FAR, PSC, and PS formed six.
2. Although four and three shape factors had grouped batches of samples into seven and six groups, respectively, the grouping of batches were not similar. It was evident that each shape factor was measuring different aspect of the shape of aggregate.

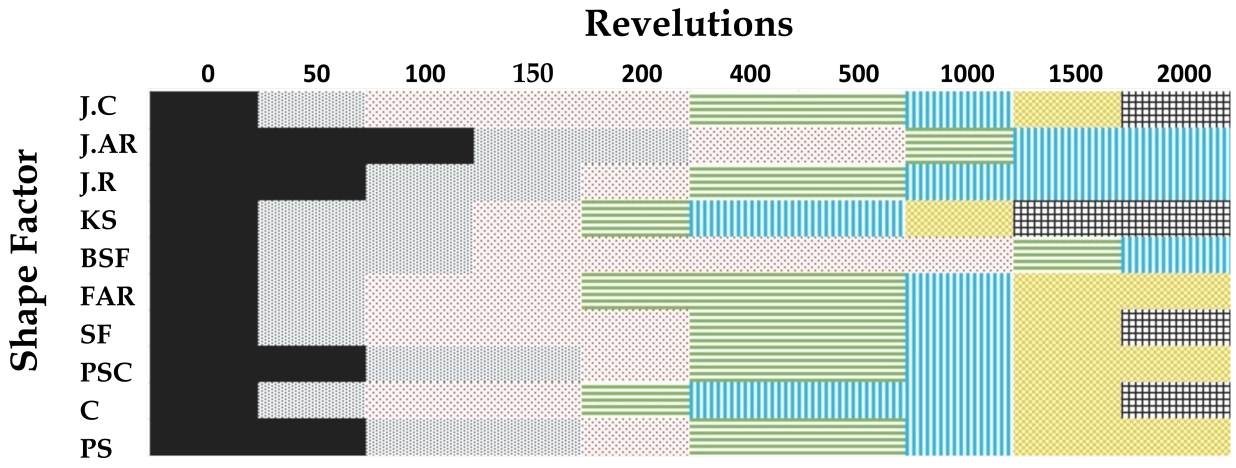

Figure 5: *Clusters as identified from ANOVA test, with ten different shape factor*

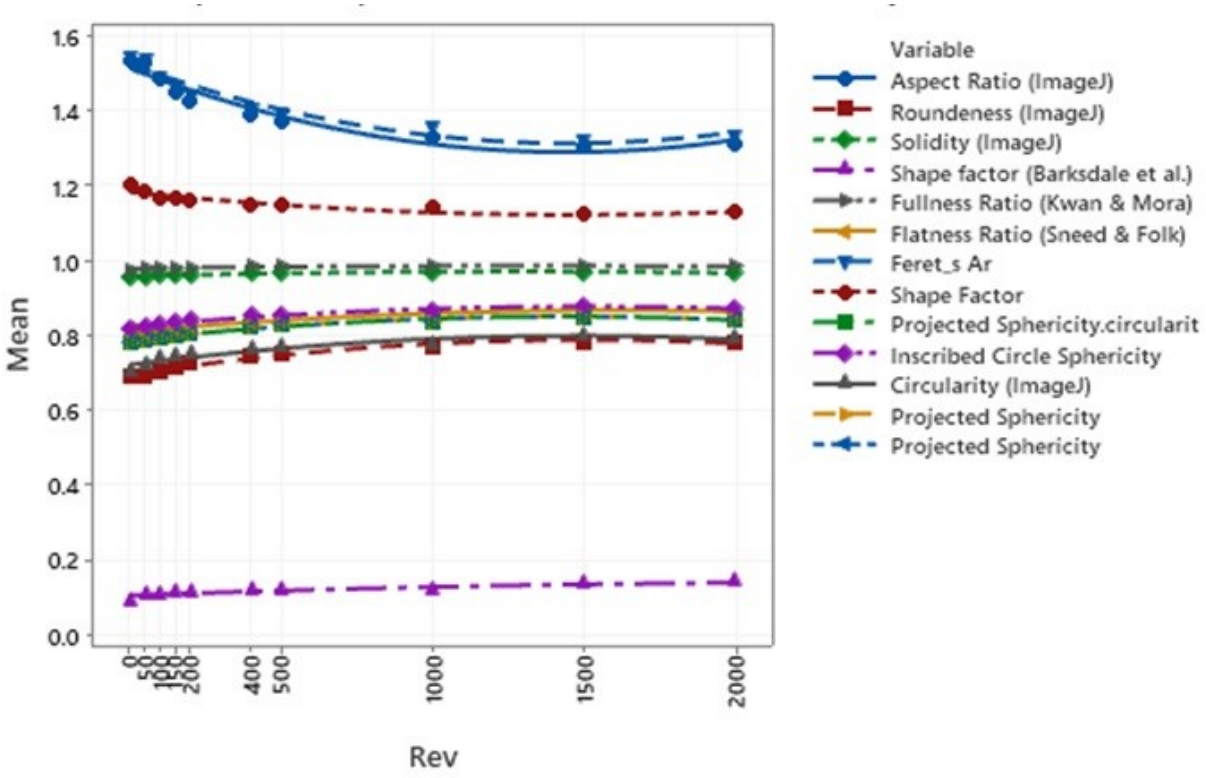

Figure 6: *Variation in mean of shape factors with revolutions*

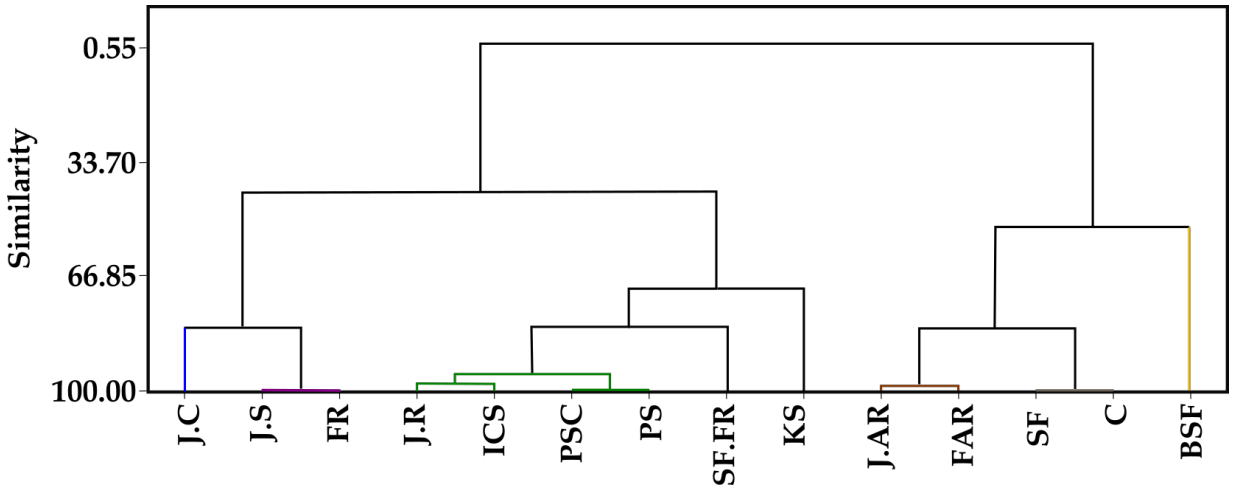

Figure 7: *Similarity of shape factors based on the cluster analysis on the aggregate shapes with labelled classes*

Table 4: *Summary of correlation coefficientcs (Pearson's Correlation) between shape factors*

	J.C	J.AR	J.R	J.S	KS	BSF	FR	SF.FR	FAR	SF	PSC	ICS	C	PS
J.C		-0.67	0.63	0.65	0.39	-0.06	0.65	0.43	-0.67	-0.99	0.76	0.66	-0.98	0.75
J.AR	-0.67		-0.96	-0.26	-0.49	0.22	-0.26	-0.65	0.98	0.66	-0.90	-0.96	0.65	-0.89
J.R	0.63	-0.96		0.24	0.49	-0.23	0.24	0.68	-0.94	-0.61	0.91	0.97	-0.59	0.91
J.S	0.65	-0.26	0.24		-0.14	-0.27	1.00	0.11	-0.25	-0.62	0.41	0.25	-0.61	0.41
KS	0.39	-0.49	0.49	-0.14		0.41	-0.14	0.56	-0.49	-0.39	0.43	0.49	-0.38	0.42
BSF	-0.06	0.22	-0.23	-0.27	0.41		-0.26	-0.48	0.22	0.06	-0.26	0.23	0.05	-0.26
FR	0.65	-0.26	0.24	1.00	-0.14	-0.26		0.11	-0.25	-0.62	0.41	0.25	-0.61	0.41
SF.FR	0.43	-0.65	0.68	0.11	0.65	-0.48	0.11		-0.65	-0.41	0.64	0.68	-0.40	0.64
FAR	-0.67	0.98	-0.94	-0.25	-0.49	0.22	-0.25	-0.65		0.66	-0.92	-0.98	0.65	-0.90
SF	-0.99	0.66	-0.61	-0.62	-0.39	0.06	-0.62	-0.41	0.66		-0.73	-0.64	1.00	-0.72
PSC	0.76	-0.90	0.91	0.41	0.43	-0.26	0.41	0.64	-0.92	-0.73		0.94	-0.71	1.00
ICS	0.66	-0.96	0.97	0.25	0.49	-0.23	0.25	0.68	-0.98	-0.64	0.94		-0.62	0.93
C	-0.98	0.65	-0.54	-0.61	-0.38	0.05	-0.61	-0.40	0.65	1.00	-0.71	-0.62		-0.70
PS	0.75	-0.89	0.91	0.41	0.42	-0.26	0.41	0.64	-0.90	-0.72	1.00	0.93	-0.70	

3. Most shape factors had small variations with number of revolutions, while J.AR and C showed higher degree of variations.In addition, other than J.AR and FAR and SF that showed decreasing trend with number of revolutions, all others had increasing trend.
4. Principal Component Analysis (PCA) was employed on a fourteen-dimensional matrix of shape factors. Remarkably, this matrix could be effectively compressed into three principal components, collectively accounting for 90% of the data's variance. The primary component, responsible for 50% of the variance, prominently featured J.AR, J.R, FAR, and ICS. Meanwhile, the secondary component, explaining 30% of the variance, was largely influenced by J.S and F.R.
5. A correlation analysis revealed significant correlation among some shape factors. Very high correlations (more than a correlation coefficient of 0.9 with 95% confidence) was observed between J.S-FR, SF-C, PSC-PS, J.AR-FAR, J.R-ICS, J.R-PSC and J.R-PS.

The findings underscore that a single shape factor is insufficient to comprehensively characterize the form of an aggregate. Moreover, not all fourteen shape factors are indispensable, given the presence of substantial correlations among some. It can be inferred that a minimum of three distinct shape factors might be necessary to adequately define the shape attributes of an aggregate.

Acknowledgment

The authors express their sincere gratitude for the support given by Department of Civil Engineering, Faculty of Engineering, University of Jaffna.

Conflicts of interest

The authors declare that there are no financial interests or non-financial conflicts or conflicts of interest related to this research that could have influenced this research.

References

[1] Faleschini, F., Zanini, M. A., Pellegrino, C., and Pasinato, S. "Sustainable management and supply of natural and recycled aggregates in a medium-size integrated plant". In: *Waste Management* 49 (2016), pp. 146–155. ISSN: 0956-053X. DOI: https://doi.org/10.1016/j.wasman.2016.01.013.

[2] Mostofinejad, D. and Reisi, M. "A new DEM-based method to predict packing density of coarse aggregates considering their grading and shapes". In: *Construction and Building Materials* 35 (2012), pp. 414–420. ISSN: 0950-0618. DOI: https://doi.org/10.1016/j.conbuildmat.2012.04.008.

[3] Wong, V. and Kwan, A. "A 3-parameter model for packing density prediction of ternary mixes of spherical particles". In: *Powder Technology* 268 (2014), pp. 357–367. ISSN: 0032-5910. DOI: https://doi.org/10.1016/j.powtec.2014.08.036.

[4] Lin, J., Chen, H., Zhang, R., and Liu, L. "Characterization of the wall effect of concrete via random packing of polydispersed superball-shaped aggregates". In: *Materials Characterization* 154 (2019), pp. 335–343. ISSN: 1044-5803. DOI: https://doi.org/10.1016/j.matchar.2019.06.024.

[5] Kusumawardani, D. and Wong, Y. "The influence of aggregate shape properties on aggregate packing in porous asphalt mixture (PAM)". In: *Construction and Building Materials* 255 (2020), p. 119379. ISSN: 0950-0618. DOI: https://doi.org/10.1016/j.conbuildmat.2020.119379.

[6] Furnas, C. *Flow of Gases Through Beds of Broken Solids*. Bulletin (United States. Bureau of Mines) nos. 307-312. U.S. Government Printing Office, 1929.

[7] Westman, A. E. R. and Hugill, H. R. "THE PACKING OF PARTICLES1". In: *Journal of the American Ceramic Society* 13.10 (1930), pp. 767–779. DOI: https://doi.org/10.1111/j.1151-2916.1930.tb16222.x. eprint: https://ceramics.onlinelibrary.wiley.com/doi/pdf/10.1111/j.1151-2916.1930.tb16222.x.

[8] Stroeven, P. and Stroeven, M. "Assessment of packing characteristics by computer simulation". In: *Cement and Concrete Research* 29.8 (1999), pp. 1201–1206. ISSN: 0008-8846. DOI: https://doi.org/10.1016/S0008-8846(99)00020-4.

[9] Hettiarachchi, H. and Mampearachchi, W. "Effect of vibration frequency, size ratio and large particle volume fraction on packing density of binary spherical mixtures". In: *Powder Technology* 336 (2018), pp. 150–160. ISSN: 0032-5910. DOI: https://doi.org/10.1016/j.powtec.2018.05.049.

[10] Kwan, A. K. H. and Mora, C. F. "Effects of various shape parameters on packing of aggregate particles". In: *Magazine of Concrete Research* 53.2 (2001), pp. 91–100. DOI: 10.1680/macr.2001.53.2.91. eprint: https://doi.org/10.1680/macr.2001.53.2.91.